Nonlinear effects in inductively coupled plasmas[a)]

A. I. Smolyakov[b)]
Department of Physics and Engineering Physics, University of Saskatchewan, Saskatoon, Saskatchewan S7N 5E2, Canada

V. A. Godyak
OSRAM SYLVANIA, 71 Cherry Hill Drive, Beverly, Massachusetts 01915

Y. O. Tyshetskiy
Department of Physics and Engineering Physics, University of Saskatchewan, Saskatoon, Saskatchewan S7N 5E2, Canada

(Received 18 November 2002; accepted 18 February 2003)

Nonlinear effects in an inductive discharge have been studied experimentally and theoretically in a low pressure and low frequency operational regime. Plasma dynamics at these conditions is strongly nonlinear due to inertial and Lorentz forces. Nonlinear plasma polarization at the second harmonic and mean (ponderomotive) potential as well as generation of the electric current at the second harmonic have been measured experimentally and analyzed theoretically. It has been found experimentally that classical expression for the ponderomotive force is not applicable for warm plasmas in the inductive discharges that are typically in the regime of the anomalous skin effect. A new expression for the ponderomotive force in a warm plasma had been derived and was shown to be in a good agreement with experimental data. The influence of nonlinear effects on the plasma heating in the low frequency regime has been investigated theoretically. © *2003 American Institute of Physics.* [DOI: 10.1063/1.1566443]

I. INTRODUCTION

Inductive rf discharges or inductively coupled plasmas (ICP) continue to attract attention as effective plasma sources in many industrial applications.[1,2] Although most practical ICP operate at 13.56 MHz, the trend to reduce the operation frequency is clearly recognizable in recent ICP developments. Application of low frequencies reduces capacitive coupling and transmission line effects and leads to simpler and lower cost rf power sources and matching circuits.

There are two important characteristic features of the ICP operating at low frequency: anomalous (noncollisional) heating and nonlinearity. Many of the applications of ICP require low-pressure regimes (with neutral gas pressure 1–10 mTorr). For a typical electron temperature of few eV the electron–neutral collision frequency ν is small, $\nu \ll \omega$ (ω is a driving rf frequency), and electrons in such a discharge are weakly collisional. In absence of collisions, the collisionless wave–particle interaction (Landau damping) becomes the main mechanism of the wave absorption and plasma heating.[3–5] When the particle thermal velocity becomes comparable with the wave phase velocity, the resonant wave–particle interaction leads to the wave damping, and the collisionless interaction becomes an effective dissipation mechanism replacing real collisions. Qualitatively, the collisionless dissipation can be described as an effective dissipation due to the resonant wave–particle Landau interaction. In a configuration of the ICP discharge, the resonance occurs when the electron spends in the skin layer the time approximately equal to the wave period, so that the resonant condition is $\omega \simeq k v_{\mathrm{th}} = v_{\mathrm{th}}/\delta$, where v_{th} is the particle thermal velocity, $\delta = 1/k$ is the skin depth width, and k is the effective wave number. Thus, the particle leaving the skin layer after the reflection from the boundary experiences the effect of the electric field that is in-phase with the electric field when the particle approaches the skin layer. Since the wave energy dissipation is mainly due to the resonant particle, the effective collision frequency is $\nu_{\mathrm{eff}} \simeq v_{\mathrm{th}}/\delta$.[6] Therefore, the absorption of the electromagnetic wave due to the interaction of the wave with warm electrons can be described by the classical skin depth expression $\delta = (c^2 \nu/\omega_{pe}^2 \omega)^{1/2}$ by replacing $\nu \to v_{\mathrm{th}}/\delta$. This results in a qualitatively correct expression for the anomalous skin depth $\delta \simeq (c^2 v_{\mathrm{th}}/\omega_{pe}^2 \omega)^{1/3}$. The regime of the anomalous skin effect,[3] when the electric current is not a local function of the electric field, is often referred to as nonlocal regime,[7–10] while the regime of the classical skin effect (highly collisional, or short mean free path regime) is referred to as a local regime.

The second important characteristic of the low frequency ICP is due to the fact that the nonlinear Lorentz force can be much larger than the force of the inductive electric field.[11] This is the regime of the electron (Hall) magnetohydrodynamics (EMHD),[12] that has been traditionally applied to fast phenomena in high power pulsed plasma systems and some magnetospheric plasmas. In ICPs nonlinear effects are small at high operation frequency. At low frequencies, the nonlinear force increases $\tilde{B} \sim \omega^{-1}$ so that $\omega_c > (\omega, \nu)$, where $\omega_c = e\tilde{B}/m_e c$ is the electron cyclotron frequency in the rf induced magnetic field $\tilde{B}$. Nonlinear forces in ICP may significantly affect plasma density profile.[13–16] They also generate higher harmonics of the electric current,[11] electrostatic potential,[17,18] and can modify the skin-effect.[19–21] In this pa-

[a)] Paper CI2 2, Bull. Am. Phys. Soc. **47**, 57 (2002).
[b)] Invited speaker.

per we review the experimental data and theoretical models describing these effects.

II. NONLINEAR FORCES IN ICP

A. Electron magnetohydrodynamic equations in ICP

In this section we qualitatively consider nonlinear effects due to the rf magnetic field (Lorentz force) and electron inertia. These forces lead to excitation of the polarization (ponderomotive and second harmonic) plasma potential and nonlinear current. In neglect of thermal effects, total nonlinear force can be obtained from the momentum equation

$$m\frac{\partial \mathbf{v}}{\partial t}+\nu m\mathbf{v}+e\mathbf{E}=-\mathbf{F}, \tag{1}$$

$$\mathbf{F}\equiv\frac{e}{c}\mathbf{v}\times\mathbf{B}+m(\mathbf{v}\cdot\boldsymbol{\nabla})\boldsymbol{v}=\frac{e}{c}\mathbf{v}\times\mathbf{B}+m\left(\nabla\frac{\mathbf{v}^2}{2}-\mathbf{v}\times\boldsymbol{\nabla}\times\mathbf{v}\right). \tag{2}$$

Assuming that ions are immobile, the electron velocity can be related to the magnetic field $\nabla\times\mathbf{B}=-4\pi en\mathbf{v}/c$. Sometimes, full (nonaveraged) $\mathbf{F}$ consisting of the time averaged and second harmonic components is referred to as a generalized ponderomotive force.[21] In what follows the ponderomotive force will refer to the dc part only.

Nonlinear current and nonlinear polarization field are created by two different components of the nonlinear force. The total nonlinear force (2) can be represented as a sum of potential and solenoidal parts

$$\mathbf{F}\equiv e\boldsymbol{\nabla}\Phi^p+\nabla\times\mathbf{G}. \tag{3}$$

The potential part is responsible for plasma polarization leading to the electrostatic field $\mathbf{E}^p=-\boldsymbol{\nabla}\Phi^p$, with Φ^p being a polarization potential, while the solenoidal part $\nabla\times\mathbf{G}$ produces a nonlinear current, where $\mathbf{G}$ is some vector potential function. Note that the potential and solenoidal components in (3) are independent of each other. Respectively, the nonlinear polarization field and nonlinear current are also independent.

It is interesting to note that potential and solenoidal parts of $\mathbf{F}$ have different scaling with collision frequency ν; the scaling may also be different for dc and second harmonic parts.[21,22] One can easily show that the solenoidal part vanishes in absence of collisions and thermal effects. Indeed, in this case, one has

$$\partial\mathbf{v}/\partial t=-e\mathbf{E}/m_e, \quad \text{or} \quad \nabla\times\mathbf{v}=e\mathbf{B}/m_ec. \tag{4}$$

Then, from Eq. (2) one obtains

$$\mathbf{F}\equiv\frac{e}{c}\mathbf{v}\times\mathbf{B}+m(\mathbf{v}\cdot\boldsymbol{\nabla})\mathbf{v}=\nabla\left(m\frac{\mathbf{v}^2}{2}\right). \tag{5}$$

This is a purely potential force which does not produce any nonlinear current. The polarization potential in this case is $\Phi^p=m\mathbf{v}^2/2$, and the nonlinear force is the gradient of the electron oscillatory energy. The contribution to the nonlinear current occurs solely due to a finite phase shift between the time derivative of the electron velocity and the electric field. Such a phase shift is a result of dissipation due to collisions or collisionless absorption associated with wave-field resonance. Collisionless absorption can be described as a viscosity effect in the momentum balance equation[23,24]

$$-i\omega\mathbf{v}=-\frac{e}{m}\mathbf{E}-\nu_{\text{eff}}\mathbf{v}, \tag{6}$$

where $\nu_{\text{eff}}=\nu+k^2\eta_{z\phi}$ includes the contribution of collisionless absorption processes accounted for via the viscosity tensor $\eta_{z\phi}$[24] One has to remember that ν_{eff} is in fact a nonlocal operator and, in general, has an imaginary part.

Note that each, the inertial $m(\mathbf{v}\cdot\boldsymbol{\nabla})\mathbf{v}$ and the Lorentz force $e\mathbf{v}\times\mathbf{B}/c$ terms, have both potential and solenoidal components. In absence of collisions, solenoidal components are cancelled completely resulting in a total force that is pure potential as in Eq. (5). In general case $\nu_{\text{eff}}\neq 0$ the solenoidal component leading to the generation of nonlinear current may remain finite. As we shall see below, two-dimensional geometry is a required condition for generation of the nonlinear current.

The potential and solenoidal components can be separated in Eq. (1) by taking $\nabla\cdot$ and $\nabla\times$ operations, respectively. Applying the $\nabla\times$ operator to equation (1) one obtains a nonlinear equation for the azimuthal magnetic field B_ϕ in a cylindrical ICP discharge with a planar coil where there are two components of the magnetic field created by the external coil, $\mathbf{B}=B_r(r,z)\hat{\mathbf{r}}+B_z(r,z)\hat{\mathbf{z}}$

$$\frac{\partial}{\partial t}B_\phi-\frac{c^2}{\omega_{pe}^2}\left(\frac{\partial}{\partial t}+\nu\right)\left(\nabla^2B_\phi-\frac{B_\phi}{r^2}\right)=\frac{c}{4\pi en_0}\left(\frac{\partial}{\partial r}K_z-\frac{\partial}{\partial z}K_r-\frac{c^2}{\omega_{pe}^2}\frac{\partial}{\partial z}\frac{1}{r}\times\left[\frac{\partial}{\partial z}B_r-\frac{\partial}{\partial r}B_z\right]^2\right). \tag{7}$$

Here $\mathbf{K}\equiv(\mathbf{B}\cdot\boldsymbol{\nabla})\mathbf{B}$ is a vector related to the curvature of the magnetic field

$$\mathbf{K}=K_r\hat{\mathbf{r}}+K_z\hat{\mathbf{z}}=\left(\frac{1}{2}\frac{\partial}{\partial r}B_r^2+B_z\frac{\partial}{\partial z}B_r\right)\hat{\mathbf{r}}+\left(\frac{1}{2}\frac{\partial}{\partial z}B_z^2+B_r\frac{\partial}{\partial r}B_z\right)\hat{\mathbf{z}}. \tag{8}$$

The right hand side of Eq. (7) is a source of the nonlinear azimuthal magnetic field B_ϕ which has time averaged (dc) and second harmonic components. Note that nonlinear current is essentially two-dimensional effect, both $B_r\neq 0$ and $B_z\neq 0$ are required to have finite B_ϕ.

To obtain the equation for the potential component of the nonlinear force, we take the divergence of the electron momentum balance (1). Taking into account that $\nabla\cdot\mathbf{v}=0$ and neglecting the effects of plasma inhomogeneities, one obtains

$$\nabla^2\Phi^p=\frac{1}{4\pi en}\left(\nabla^2\frac{B^2}{2}-\nabla\cdot\mathbf{K}-\frac{c^2}{\omega_{pe}^2}\frac{\partial}{r\partial r}\left[\frac{\partial B_z}{\partial r}-\frac{\partial B_r}{\partial z}\right]^2\right). \tag{9}$$

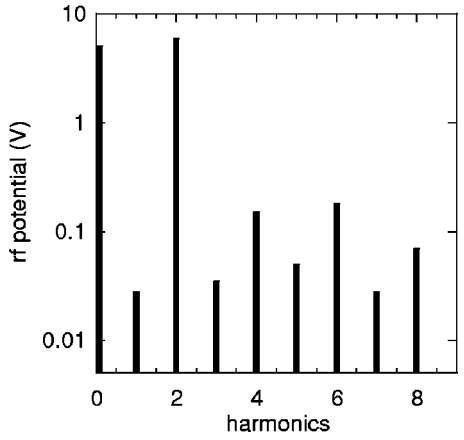

FIG. 1. The frequency spectrum of the polarization potential in the middle of the skin layer, at a distance of 1 cm from the quartz window ($z=1$ cm, $r=4$ cm) in an ICP driven at 0.45 MHz.

The $\nabla^2 B^2/2$ and $\nabla\cdot\mathbf{K}$ terms in this equation are due to the Lorentz force, while the last term is due to the inertial force. Both dc and second harmonic components of the nonlinear polarization field are generated. The first and third terms in Eq. (9) produce the dc and second harmonic potential that are equal in the amplitude, while the dc and second harmonic generated by the second term (due to **K**) may be different. The curvature term ($\nabla\cdot\mathbf{K}$) is small when $\delta<R$, so one can expect that the dc and the second harmonic potential in ICP will be comparable in amplitude as it is confirmed in the experiment (see Fig. 1 and the next section).

Essentially, the role of the electrostatic polarization field is to balance the nonlinear Lorentz and the inertial forces.[13] It can be simply illustrated for an infinite in z-direction cylindrical ICP. In this case all forces are in radial direction, so that the radial component of the polarization field can be written as

$$E_r^p = -\frac{1}{c}B_z v_\phi + \frac{m_e}{e}\frac{v_\phi^2}{r} = -\frac{1}{4\pi n_0}\frac{\partial}{\partial r}\frac{B_z^2}{2} + \frac{1}{4\pi n_0}\frac{c^2}{\omega_{pe}^2}\frac{1}{r}\left(\frac{\partial B_z}{\partial r}\right)^2. \tag{10}$$

The latter equality in (10) is obtained by using the Ampère law $\nabla\times\mathbf{B}=-4\pi e n\mathbf{v}/c$. This expression corresponds to the first and the last terms in Eq. (9). Note that in an infinite cylindrical ICP $\mathbf{K}=\mathbf{0}$. The contribution of the inertial term [the last term in (10)] is typically small in the nonlocal regime, because

$$\frac{c^2}{\omega_{pe}^2\delta^2} = \frac{c^2 v_{\mathrm{th}}/\omega}{\omega_{pe}^2\delta^3}\frac{\delta}{v_{\mathrm{th}}/\omega} = \frac{\delta}{v_{\mathrm{th}}/\omega} < 1, \tag{11}$$

and the width of the skin layer is much smaller than the ICP radius, $\delta<R$.

The nature of nonlinear polarization fields in inductively coupled plasma is closely related to the Hall drift of electrons in the rf magnetic field. In presence of the magnetic field, the total electron current can be written in the form $\mathbf{J}=\sigma_P\mathbf{E}+\sigma_H\mathbf{E}\times\mathbf{b}$, where $\mathbf{b}=\mathbf{B}/B$ is the unit vector along the magnetic field, σ_P is the Pedersen conductivity along the electric field, and σ_H is the Hall conductivity in the direction perpendicular to both the electric and magnetic field.[25] The primary electric field E_ϕ creates a Hall current in the radial direction. To compensate this current and maintain $J_r=0$ a finite radial electric field E_r must be generated. This is the polarization field.

A corollary to this result is an interesting fact that, in an infinite ICP, the effects of the magnetic field (including those from the external dc magnetic field) do not modify the penetration of the rf field into the plasma.[18] Though σ_P is modified by the magnetic field, this modification is compensated by the Hall current from the induced radial polarization field E_r^p, so that the net current in the $\hat{\boldsymbol{\phi}}$ direction is not changed

$$v_\phi = -\frac{e}{m}\frac{E_\phi(-i\omega+\nu)+E_r^p eB_z/m_e c}{(eB_z/m_e c)^2+(-i\omega+\nu)^2} = -\frac{e}{m}\frac{E_\phi}{(-i\omega+\nu)}. \tag{12}$$

In the result, in an infinite ICP, the magnetic field does not change the skin effect.[18,21] In a finite length ICP, when there is inhomogeneity in the z direction, the situation may be different.[21]

B. Experimental observations of nonlinear polarization field and electric current

Experiments have been carried out in a cylindrical low pressure argon ICP, with a metallic chamber with diameter 2R=20 cm and length L=10.5 cm, and a quartz window separating a planar coil from plasma, as described in detail in Ref. 26. To enhance nonlinear processes the driving frequency and gas pressure were reduced, correspondingly, to 0.45 MHz and 1 mTorr.

The rf discharge was maintained at a discharge power $P=200$ W. The basic plasma parameters: n_e, T_e, the rf and dc plasma potential have been measured with a Langmuir probe moved along the axial (z) direction. Nonlinear harmonics of the electrostatic potential were directly obtained from Langmuir probe measurements. The ponderomotive potential was calculated from the dc potential and plasma density data as decribed in Sec. IV. Measurements were made on the discharge axis ($r=0$) and at a fixed radial position $r=4$ cm, which corresponds to the maxima of the radial distribution of the azimuthal rf electric field $E(r)$ and the radial magnetic field $B_r(r)$. The electron–atom collision frequency ν was found by using Langmuir probe data and argon cross sections. The electromagnetic fields $E(r)$ and $B_r(r)$ and the plasma current density distributions J_θ, J_r, and J_z were inferred from magnetic probe measurement made along the axial direction at $r=4$ cm and along the radial direction at $z=3.2$ cm. Langmuir and magnetic probe measurement were made over a wide frequency range (0.45–13.56 MHz) but here we mainly consider data for $\omega/2\pi=0.45$ MHz where nonlinear effects are largest.

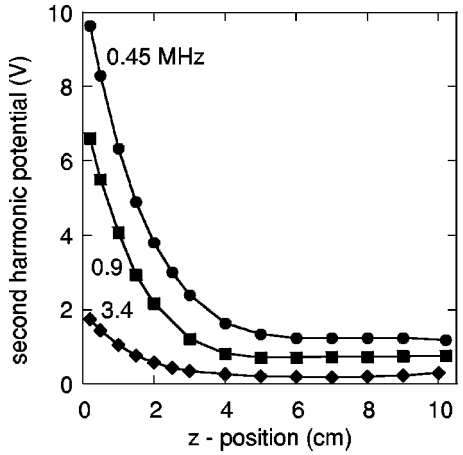

FIG. 2. The second harmonic plasma potential spatial profiles for three different driving frequencies: $f=0.45$, 0.9, and 3.4 MHz.

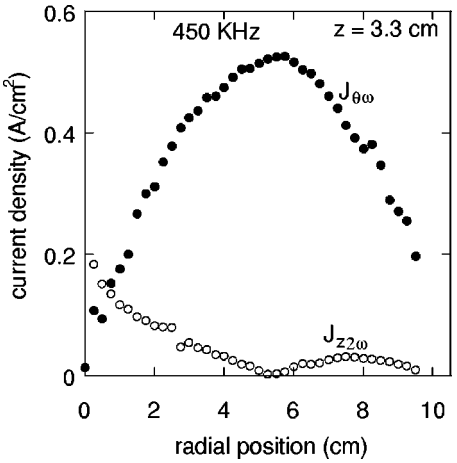

FIG. 3. The axial current $J_{z2\omega}$ at the second harmonic measured at $f=0.45$ MHz and 1 mTorr. The azimuthal primary harmonic current $J_{\theta\omega}$ is shown for comparison.

1. Nonlinear polarization potential

To our knowledge, the nonlinear polarization potential has not been observed in experiments with inductive discharges. One reason for this was that for a typical ICP driven at 13.56 MHz nonlinear effects are negligibly small. They are significantly increased for lower frequency. Note that lower frequencies correspond to the stronger anomalous skin effect, $\omega < v_{\mathrm{th}}/\delta$.

The frequency spectrum of the plasma potential in the middle of the skin layer, close to the quartz window ($z=1$ cm, $r=4$ cm) in an ICP driven at 0.45 MHz, is shown in Fig. 1. Note that dc plasma potential (zero frequency, $\omega=0$) has been deduced from the plasma density and plasma potential profiles while the oscillating rf harmonics ($\omega, 2\omega, 3\omega, \ldots$) were measured directly. The dc potential corresponds to the nonlinear ponderomotive force and will be further described in Sec. III. As it is seen in Fig. 1, the first (fundamental) harmonic, probably induced by finite capacitive coupling from the induction coil, is smallest, while the second harmonic exceeds the electron temperature and dominates all others. Note that the fundamental harmonic shown in Fig. 1 is the harmonic of the *electrostatic potential* and it is different from the fundamental harmonic in *the inductive electric field*. The fundamental harmonic of the electrostatic potential is the result of the parasitic (capacitive) coupling and in the ideal ICP should not appear. Figure 1 also shows that all even harmonics are significantly larger than odd harmonics. The nonlinear polarization potential at the second harmonic is approximately equal to the dc part of potential that indicates that the curvature produced potential is small [see Eq. (9) and the discussion above in Sec. II A]. Amplitudes of the second harmonic and dc (ponderomotive) potential should be approximately equal when the dissipation is small.[21,22]

The axial distribution of the second harmonic potential at $r=4$ cm is shown in Fig. 2 for argon pressure of 1 mTorr and three driving frequencies of 0.45, 0.9, and 3.4 MHz. The second harmonic voltage drops sharply inside the plasma thus suggesting that the source is located in the skin layer where the electric and magnetic field are strongest. As noted above, the dc and second harmonic polarization potentials are approximately equal and have similar spatial profiles. The experimental profile of the ponderomotive potential is discussed in Sec. III where it is also compared with a theoretical model.

The second harmonic potential decreases strongly with an increase in gas pressure and driving frequency. This trend is consistent with the nonlinear nature of the polarization field. Indeed, with growing gas pressure, the discharge ionization and energy balance require a smaller rf electric field and a smaller drift velocity, while with increasing frequency a smaller magnetic rf field is required to induce the same rf electric field.

Measurements performed at different frequencies and over a wide range of the discharge power have shown that the second harmonic voltage generated in the skin layer depends very little on the discharge power (plasma density). Thus, at 1 mTorr and driving frequency 0.9 MHz, the change in the discharge power from 50 to 400 W has resulted in a change of $V_{2\omega}$ from 5 to 8 Volts. This is consistent with a weak dependence of the primary rf electric field with the discharge power.[10] In a steady-state weakly ionized gas discharge plasma, the rf electric field and the electron drift velocity are held almost constant by the ionization and electron energy balance.[10]

2. Nonlinear currents at the second harmonics

Second harmonic current $J_{2\omega}$ induced by the rf Lorentz force and circulating around the main discharge current has been found in our ICP operating at 6.78 and 3.39 MHz.[11,27] The axial and radial components of $J_{2\omega}$ measured at 0.45 MHz and 1 mTorr are shown in Figs. 3 and 4.

The space dependence of both second harmonic components shown in Figs. 3 and 4 are similar to those found in Ref. 11 for high frequency. The relative magnitude of $J_{2\omega}$ at 0.45 MHz was found to be larger than that of at higher frequencies in Ref. 11. Our measurements show that the $J_{2\omega}$ at 0.9 MHz is comparable to that of at 0.45 MHz, so that the

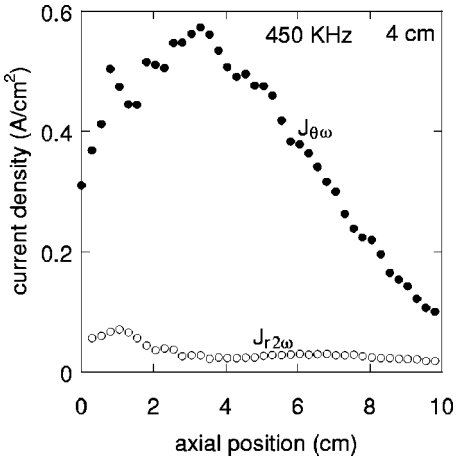

FIG. 4. The radial current $J_{r2\omega}$ at the second harmonic measured at $f=0.45$ MHz and 1 mTorr. The azimuthal primary harmonic current $J_{\theta\omega}$ is shown for comparison.

frequency dependence at low frequencies is much weaker than that of at higher frequencies in Ref. 11 where $J_{2\omega}$ is nearly proportional to ω^{-1}.

In a cylindrical ICP with a flat coil, there are two components of rf magnetic field: B_z and B_r. As shown in Refs. 11 and 18 and as follows from Eq. (7), the second harmonic current is essentially a two-dimensional effect caused by the rf magnetic field curvature $\mathbf{K}=\mathbf{B}\cdot\nabla\mathbf{B}$. The main contribution comes from the Lorentz force while the contribution of the inertial term is small [see Eq. (11)]. The Lorentz force drives nonlinear currents along closed paths in the $z-r$ plane forming a poloidal current structure resulting in $J_{2\omega}$ maximum at the discharge axis. Note that the current density $J_{2\omega}$ is not a local function of the Lorentz force, but is defined by the total plasma impedance and by the Lorentz force integrated along a closed current path as well as boundary conditions.

III. PONDEROMOTIVE FORCE IN A WARM PLASMA

Ponderomotive force is an effect of a dc component of the nonlinear polarization potential. Attempts over the last 30 years to demonstrate a ponderomotive effect in a collisional, weakly ionized, gas discharge plasma have failed because the ionization and energy balance of a weakly ionized plasma limits the electric field and electron drift velocity to a low level insufficient for a significant ponderomotive effect. Recent advances in inductively coupled plasma (ICP) sources for plasma processing of semiconductors and lighting technology led to the development of ICPs maintained at an extremely low gas pressure with an electron oscillatory energy approaching the electron thermal energy. Under such conditions, the interaction of electrons with the electromagnetic field becomes strongly nonlocal due to the electron thermal motion that results in the anomalous skin effect. In the regime of the anomalous skin effect, the electron drift velocity is not a local function of the rf field, and the classical expression for the ponderomotive (Miller) force[28]

$$F=-\nabla U_M, \quad U_M=eE_\phi^2/2m_e(\omega^2+\nu^2), \tag{13}$$

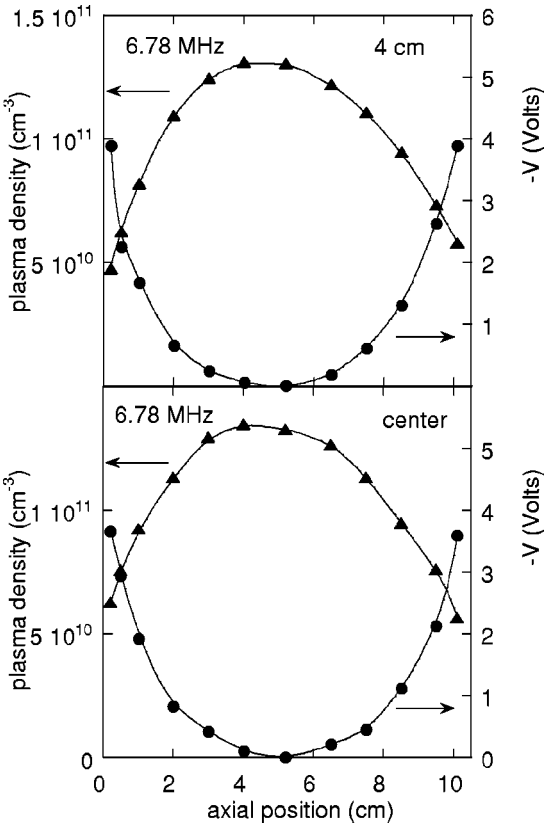

FIG. 5. The plasma density $n(z)$ and the ambipolar potential $V(z)$ profiles, measured in an ICP driven at 6.78 MHz, at different radial positions: $r=0$ (no rf fields) and $r=4$ cm (maximum rf field amplitude). Note that the negative $-V(z)$ potential is shown.

derived in the local approximation is no longer valid.[16,27,29] In earlier studies of the ponderomotive force[30–35] the effects of thermal motion were considered as small corrections (for $\omega\gg kv_{th}=v_{th}/\delta$) to cold plasma expression.[28] It turns out that in the anomalous skin effect regime, when $\omega\ll v_{th}/\delta$, resonant wave–particle interaction also strongly affects the ponderomotive force in addition to the modification of plasma heating.[36–40]

A significant deviation of the ponderomotive force in a warm plasma from the classical result was found recently in experiments.[16,29] The plasma density $n(z)$ and the ambipolar potential $V(z)$ profiles, measured at different radial positions, are shown in Figs. 5 and 6 at 6.78 and 0.45 MHz, respectively. At 6.78 MHz, at the center and at a radius of 4 cm the measured $n(z)$ and $V(z)$ are rather symmetrical about discharge mid-plane and have a Boltzmann distribution $n(z)/n_0=\exp(eV(z)/T_e)$. The spatial distributions of $n(z)$ and $V(z)$ are typical for low pressure ICPs found in the literature.

A significant asymmetry in the plasma density and the plasma potential profiles is seen at 0.45 MHz in Fig. 6 for both radial positions. At the radial position $r=4$ cm, where $E(r)$ and $B_r(r)$ are peaking, there is a significant shift in z position between the maximum of n (at $z\simeq 5.5$ cm) and the minimum of V (at $z\simeq 2.1$ cm) and there is a clear reduction in plasma potential and plasma density at the left (coil) side boundary. At the plasma axis ($r=0$) where both $E(r)$, and $B_r(r)$ are zero, the maximum in $n(z)$ coincides with mini-

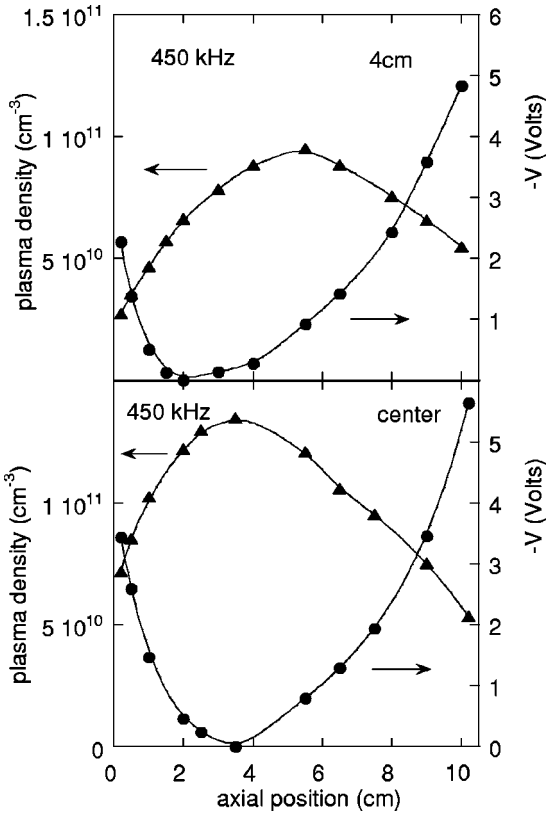

FIG. 6. The plasma density $n(z)$ and the ambipolar potential $V(z)$ profiles, measured in an ICP driven at 0.45 MHz, at different radial positions: $r=0$ (no rf fields) and $r=4$ cm (maximum rf field amplitude).

mum in $V(z)$. The difference in position between the plasma density and the potential profiles is caused by the ponderomotive force, which can be accounted for in the plasma equilibrium equation. The ponderomotive potential force $en\nabla U$ can be calculated as a difference between the pressure gradient force and the force due to the bulk plasma potential V, $T_e\nabla n-en\nabla V-en\nabla U=0$. The axial distributions of the measured plasma electrical potential V and the effective thermal potential $T_p=T_e/e\ln n$ are shown in Fig. 7 for both radial positions. An essential difference between T_p and V in the skin layer is seen for $r=4$ cm, while $T_p=V$ everywhere along the plasma central axis. The ponderomotive potential $U_{\exp}$ calculated as a difference between T_p and V is shown in Fig. 8 along with the U_M potential of (13) calculated with the experimental value of E_ϕ. There is a significant discrepancy between $U_{\exp}=T_p-V$ and the Miller ponderomotive potential U_M. It was found[41] that in the regime $v_{\rm th}/\omega\delta>1$ the magnitude of the ponderomotive force is strongly reduced due to the effects of particle thermal motion.

A new expression for the ponderomotive force accounting for the effects of thermal motion was derived.[41] We used a model case of a semi-infinite plasma occupying region $z>0$ with specular particles reflection at the plasma boundary $z=0$ and assuming exponential spatial dependence for the electric field, $E_y(z)=E_0\exp(-\gamma z)\exp(-i\omega t)$. Such a model gives a reasonably accurate description of the electromagnetic field in the skin layer of an inductively coupled discharge. Here E_0 is wave amplitude at $z=0$, and γ is the

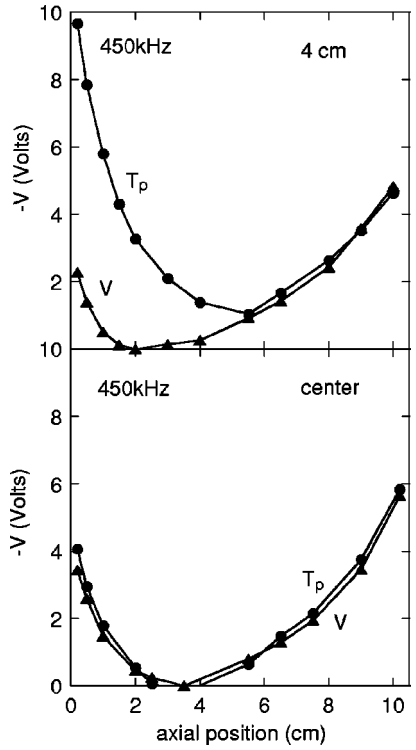

FIG. 7. The axial distribution of the measured plasma electrical potential V and the thermal potential T_p at different radial positions: $r=0$ (center) and $r=4$ cm.

complex wavevector $\gamma=1/\delta-i\varkappa$. In this model, the ponderomotive force F_p is in z direction and given by the following expression:

$$F_p=\frac{1}{2c}\mathrm{Re}\{J_yB_x^*\}=\frac{\omega_{pe}^2}{8\pi\omega}E_0^2\exp\left(-\frac{2z}{\delta}\right)\mathrm{Re}\left[i\frac{\gamma^*}{\gamma v_{\rm th}}(Z(-is)-\exp(\gamma z)G(\gamma z,s))\right]. \quad (14)$$

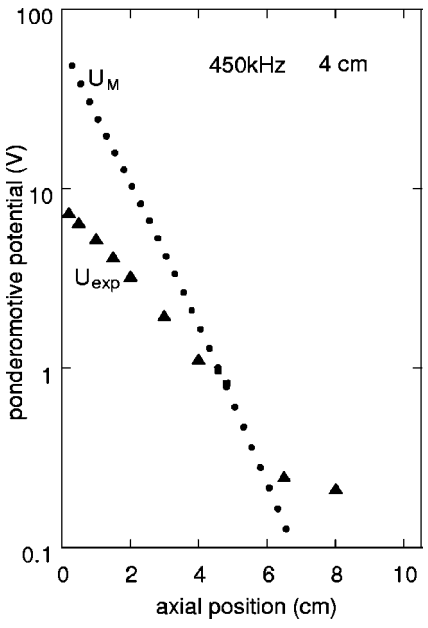

FIG. 8. The ponderomotive potential $U_{\exp}$ evaluated from Fig. 7 as the difference between T_p and V, shown together with the Miller potential U_M.

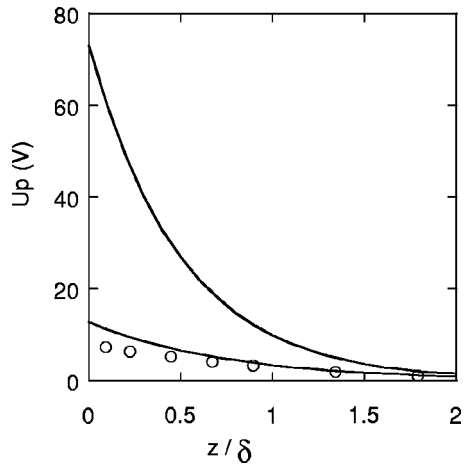

FIG. 9. Absolute value of the ponderomotive potential calculated from the linear theory for $f=0.45$ MHz for local ($T_e=0$) and nonlocal ($T_e=7$ eV) regimes. Other parameters are: $\nu=4\times10^6$ s^{-1}, $\delta=2.24$ cm, $E_0=1.87$ V/cm. The experimental data from Ref. 29 for $f=0.45$ MHz and $T_e=7$ eV are shown by circles.

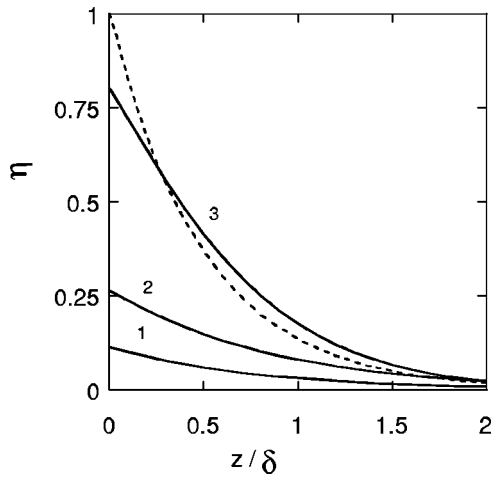

FIG. 10. Thermal reduction of the ponderomotive force in plasma at different driving frequencies: $f=0.45$ MHz (curve 1), $f=2$ MHz (curve 2), and $f=13.56$ MHz (curve 3). The ponderomotive force is normalized to the classical value at $T_e=0$ and $z=0$; the dashed line corresponds to the Miller force in a cold plasma ($T_e=0$).

Here $Z(p)=1/\sqrt{\pi}\int_{-\infty}^{\infty}\exp(-x^2)dx/(x-p)$ is the plasma dispersion function, and $G(z)$ is a complex function of z

$$G(\gamma z,s)=\frac{2}{\sqrt{\pi}}\int_0^{\infty}\frac{t\exp(i\gamma zs/t-t^2)}{t^2+s^2}dt.$$

The parameter $s=(\omega+i\nu)/\gamma v_{\mathrm{th}}$ describes the degree of nonlocality of the plasma;[3] $|s|=1$ separates local (classical) ($|s|>1$) and nonlocal (anomalous) ($|s|<1$) regimes of ICP. Note that in this one-dimensional model, the inertial force does not contribute to the ponderomotive force.

In the strongly nonlocal regime $s\ll1$ and assuming weak dissipation $\varkappa\delta\ll1$ one can derive from (14) the following expression for the ponderomotive force near the plasma boundary ($z=0$):

$$F_p\simeq\frac{\omega_{pe}^2}{8\pi\omega^2}E_0^2\frac{\sqrt{\pi}\omega}{v_{\mathrm{th}}}. \tag{15}$$

Note that the expression for the ponderomotive force in the nonlocal regime can be cast in a form similar to that of the local case, i.e., $F_p\simeq\omega_{pe}^2E_0^2/8\pi\delta\omega^2$, where the characteristic gradient length of the electric field δ is replaced with the characteristic length of the particle excursion over the wave period, $\delta\to\delta_{\mathrm{th}}=v_{\mathrm{th}}/\sqrt{\pi}\omega$.

In Fig. 9 we show the theoretical and experimental (shown by circles) values of the ponderomotive potential U_p for $f=0.45$ MHz. The theoretical value of the ponderomotive potential U_p is calculated from (14) by using the relation $en_0U_p=-\int_{-\infty}^{z}F_pdz$. Our model shows a significant reduction of the ponderomotive force in hot plasmas due to the particle thermal motion. For our calculations in Fig. 9 we used experimental values $\delta=2.24$ cm, $\varkappa\delta=0.1$ and $E_0=1.87$ V/cm.[16,29]

The reduction of the ponderomotive force due to the finite electron temperature becomes weaker for higher frequencies (larger values of s). In Fig. 10 we show the reduction of the ponderomotive force in nonlocal regime for three different frequencies. The parameter η is defined as a ratio of the nonlocal ponderomotive for $T_e=7$ eV to its value for $T_e=0$ at the same frequency. A thermal reduction of the ponderomotive force, that is significant for low frequencies, is very weak for the common in industrial applications frequency 13.56 MHz for which the absolute value of the ponderomotive force is negligibly small.

IV. PLASMA HEATING IN THE ANOMALOUS REGIME AT LOW FREQUENCIES

The resonant absorption of the electromagnetic wave due to the electron thermal motion is an underlying heating mechanism of the inductively coupled plasma discharge (ICP) operating in the regime of the anomalous skin effect. The latter regime occurs for $v_{\mathrm{th}}/\delta\geqslant\omega$ and $v_{\mathrm{th}}/\delta>\nu$. It has been shown[27,36] that in the low pressure ICP operating in the anomalous regime the power absorption due to the interaction with thermal electrons significantly exceeds the collisional absorption. There is an optimal frequency when the power absorption reaches the maximal value. As it was discussed in the Introduction, the resonant frequency is $\omega\simeq v_{\mathrm{th}}/\delta$. Note that in this paper we are considering only a model case of a semi-infinite plasma where there is only a single reflection from the plasma boundary. The multiple reflections of electrons from the back wall of the chamber introduce additional resonances[37] which occur at much lower frequencies $\Omega_n=v_{\mathrm{th}}/nL$ and are not considered here, where L is the size of the chamber.

It has been shown earlier that for low driving frequencies ($\omega<\nu$) and low collisionality ($\nu\leqslant v_{\mathrm{th}}/\delta$) the effects of the particle thermal motion reduce the absorption below the collisional value.[38] This effect is illustrated in Fig. 11. Note that in the region of low frequencies the total power absorbed in plasma is smaller than the collisional power S_{coll},

$$S_{\mathrm{coll}}=\frac{e^2n_0}{4m_e}E_0^2\delta\frac{\nu_{en}}{\nu_{en}^2+\omega^2}. \tag{16}$$

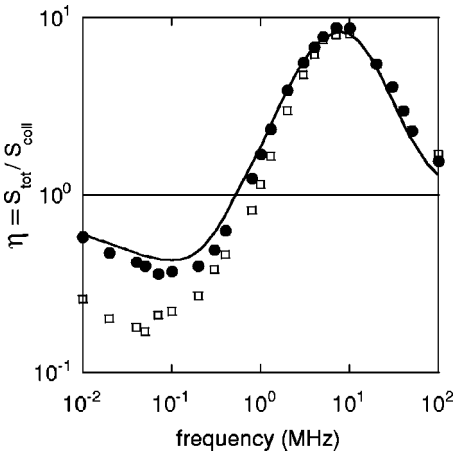

FIG. 11. Ratio of the total to collisional absorbed power. Solid curve represents the linear theory (without rf magnetic field), circles—the result of PIC simulation without rf magnetic field, squares—the PIC simulation with rf magnetic field. The parameters are: $E_0=0.5$ V/cm, $T_e=10$ eV, $n_0=2.7\times10^{10}$ cm^{-3}, $\nu=1.5\times10^6$ s^{-1}.

Nonlinear effects that are most important for low frequencies may further affect plasma heating.[13,20,39,40] We investigate these effects via direct numerical simulations of plasma heating.

To compare the results of nonlinear simulations with linear theory we use the model similar to that of Sec. III. The spatial profile of the power absorption $w(z)\equiv 1/2\,\mathrm{Re}(J_y E_y^*)$ was obtained in Ref. 38

$$w(z)=\frac{e^2 n_0}{2m_e}E_0^2\,\mathrm{Re}\left[\frac{1}{\gamma v_{\mathrm{th}}}\left(G(z)\exp(-\gamma^* z)-\exp\left(-\frac{2z}{\delta}\right)Z(-is)\right)\right]. \tag{17}$$

The total power absorbed by discharge plasma $S_{\mathrm{tot}}=\int_0^\infty w(z)dz$ is

$$S_{\mathrm{tot}}=\frac{e^2 n_0}{2m_e}E_0^2\,\mathrm{Re}\left[\frac{1}{\gamma v_{\mathrm{th}}}\left(\frac{2}{\sqrt{\pi}}\int_0^\infty \frac{t^2\exp(-t^2)}{t^2+s^2}\frac{1}{\gamma^* t - i\gamma s}\times dt-\frac{\delta}{2}Z(-is)\right)\right]. \tag{18}$$

In a cold plasma limit this expression reduces to S_{coll} (16). The ratio $\eta=S_{\mathrm{tot}}/S_{\mathrm{coll}}$ is used as a measure of the influence of the electron thermal motion on the electron heating. In numerical calculations the measured absorbed power is averaged over the rf field period.

The nonlinear effects of the rf magnetic field reduce plasma heating. This effect is illustrated in Fig. 11 which shows the results of particles-in-cell (PIC) simulations of the electron heating in a semi-infinite ICP model with an exponential spatial profile of the electromagnetic field. The simulations included electron–atom collisions (implemented into the PIC code with a direct Monte Carlo method) and the electron–electron collisions (implemented via the Langevin equation[42]) as a mechanism for the ''Maxwellization'' of the electron distribution function. The influence of the nonlinear Lorentz force can be characterized by a magnitude of the parameter ω_c/ω. For small ω_c/ω the effect of the rf magnetic field is small. For lower driving frequency, the parameter ω_c/ω is larger and the ponderomotive force becomes significant. At low frequency there is significant reduction of plasma heating due to the rf magnetic field. Expulsion of electrons from the skin layer by the ponderomotive force leads to the reduction of plasma heating.[13,39]

V. SUMMARY

Our experiments with ICPs at various rf and argon pressure have shown that nonlinear effects induced by the Lorentz force are negligible at high rf and high gas pressure. On the contrary, nonlinear effects, such as, polarization potential, the electric current at the second harmonic, and ponderomotive modification of plasma density are well pronounced in ICPs at low gas pressure and at low frequency. This corresponds to a condition where strong nonlocal $v_{\mathrm{th}}/\delta \gg (\omega,\nu)$ and strong nonlinear $\omega_c \gg (\omega,\nu)$ effects occur simultaneously. Our theoretical analysis has shown that strong rf magnetic field further reduces the electron heating at low frequencies.

We have analyzed the structure of the nonlinear forces in the ICP. We have shown that both Lorentz and inertial components have potential and solenoidal parts. The potential part leads to plasma polarization, while the solenoidal part is responsible for generation of the nonlinear electric current. Both polarization (electrostatic) potential and the nonlinear current have the time averaged (dc) and oscillating (ac, 2ω) components.

We have investigated the influence of the particle thermal motion on the ponderomotive force. In low collisional, nonlocal regimes with $v_{\mathrm{th}}/\delta \gg \omega$, the value of the ponderomotive force is strongly reduced compared to that given by the standard expression. It is interesting that low temperature ICP gave the first example of a medium where the effect of a finite electron temperature on the ponderomotive force is imporant and has been measured, while in high temperature cases such as laser or rf heated magnetically confined plasmas the ponderomotive force can generally be described by the standard Miller expression. The reduction of the ponderomotive force occurs in the regime when the particle thermal velocity exceeds the characteristic phase velocity, $v_{\mathrm{th}} \geqslant \omega/k$. Such a situation hardly can occur for propagating electromagnetic waves whose phase velocity is close to the speed of light, but it naturally occurs in the ICP when the wave is evanescent and $\omega/k=\omega\delta \ll \omega/k_0=c$, where k_0 is a vacuum wave number. (The characteristic phase velocity for the evanescent wave is the phase velocity of the characteristic Fourier component, $k=1/\delta$.) One can expect that similar reduction will occur for the laser beam penetration in the overdense plasma or in a magnetized plasma with much reduced wave phase velocity.

We have derived a new expression for the ponderomotive force in hot plasmas that is in reasonable agreement with the experimental data.[41] The modification of the ponderomotive force due to thermal effects has to be taken into account in numerical models of inductively coupled discharges.

ACKNOWLEDGMENTS

This research was supported in part (A.S. and Y.T.) by the Natural Sciences and Engineering Research Council of Canada. V.G. would like to thank R. B. Piejak and B. M. Alexandrovich for many contributions to study of nonlinear effects in ICP at OSRAM SYLVANIA Research Center.

[1]M.A. Lieberman and A.J. Lichtenberg, *Principles of Plasma Discharges and Materials Processing* (Wiley, New York, 1994).
[2]D.O. Wharmby, in *Lamps and Lighting*, edited by J.R. Coaton and A.M. Marsden (Arnold and Contributors, London, 1997).
[3]E.S. Weibel, Phys. Fluids **10**, 741 (1970).
[4]M. Lieberman and V.A. Godyak, IEEE Trans. Plasma Sci. **26**, 955 (1998).
[5]V.A. Godyak and V.I. Kolobov, Phys. Rev. Lett. **79**, 4589 (1997).
[6]B.B. Kadomtsev and O.P. Pogutse, Sov. Phys. JETP **39**, 269 (1984).
[7]V.A. Godyak, R.B. Piejak, and B.M. Alexandrovich, Plasma Sources Sci. Technol. **3**, 169 (1994).
[8]I.D. Kaganovich, V.I. Kolobov, and L. Tsendin, Appl. Phys. Lett. **69**, 3818 (1996); I.D. Kaganovich and L. Tsendin, IEEE Trans. Plasma Sci. **20**, 86 (1992).
[9]V.I. Kolobov and D.J. Economou, Plasma Sources Sci. Technol. **6**, R1 (1999).
[10]V. A. Godyak, ''Electron Kinetic and Electrodynamic Characteristics of ICP in Stochastic Heating Regime'' in *Electron Kinetics and Application of Glow Discharges*, edited by U. Kortshagen and L.D. Tsendin (Plenum, New York, 1998), pp. 241–255.
[11]V.A. Godyak, R.B. Piejak, and B.M. Alexandrovich, Phys. Rev. Lett. **83**, 1610 (1999).
[12]A.V. Gordeev, A.S. Kingsep, and L.I. Rudakov, Phys. Rep. **243**, 215 (1994).
[13]R.H. Cohen and T.D. Rognlien, Phys. Plasmas **3**, 1839 (1996); R.H. Cohen and T.D. Rognlien, Plasma Sources Sci. Technol. **5**, 442 (1996).
[14]G. DiPeso, T.D. Rognlien, V. Vahedi, and D.W. Hewett, IEEE Trans. Plasma Sci. **23**, 550 (1995).
[15]J.C. Helmer and J. Feinstein, J. Vac. Sci. Technol. B **12**, 507 (1994).
[16]V. Godyak, R. Piejak, B. Alexandrovich, and A. Smolyakov, Plasma Sources Sci. Technol. **10**, 459 (2001).
[17]V.A. Godyak, R.B. Piejak, B.M. Alexandrovich, and A.I. Smolyakov, Plasma Sources Sci. Technol. **9**, 541 (2000).
[18]A.I. Smolyakov, V. Godyak, and A. Duffy, Phys. Plasmas **7**, 4755 (2000).
[19]M. Tuszewski, Phys. Rev. Lett. **77**, 1286 (1996).
[20]J.D. Evans and F.F. Chen, Phys. Rev. Lett. **86**, 5502 (2001).
[21]F. F. Chen, Phys. Plasmas **8**, 3008 (2001).
[22]R.B. Piejak and V.A. Godyak, Appl. Phys. Lett. **76**, 2188 (2000).
[23]M.M. Turner, Phys. Rev. Lett. **75**, 1312 (1995).
[24]E. Furkal and A. Smolyakov, Phys. Plasmas **7**, 122 (2000).
[25]S. I. Braginskii, in *Reviews of Plasma Physics*, edited by M.A. Leontovich (Consultants Bureau, New York, 1965), Vol. 1, p. 214.
[26]V.A. Godyak, R.B. Piejak, and B.M. Alexandrovich, J. Appl. Phys. **85**, 703 (1999).
[27]V.A. Godyak, R.B. Piejak, B.M. Alexandrovich, and V.I. Kolobov, Phys. Plasmas **6**, 1804 (1999).
[28]E.V. Gaponov and M.E. Miller, Sov. Phys. JETP **25**, 952 (1958).
[29]V.A. Godyak, Bulg. J. Phys. **27**, 1319 (2000).
[30]R.E. Aamodt and M.C. Vella, Phys. Rev. Lett. **39**, 1273 (1977).
[31]H. Schamel and G. Schmidt, J. Plasma Phys. **24**, 149 (1980); H. Schamel, Phys. Rev. Lett. **20**, 1339 (1979).
[32]P. Mora and R. Pellat, Phys. Fluids **22**, 2408 (1979); **24**, 2219 (1981).
[33]G. Schmidt, Phys. Lett. A **74**, 222 (1979).
[34]I.D. Kaganovich, Tech. Phys. Lett. **19**, 276 (1993).
[35]T.W. Johnston, RCA Rev. **17**, 571 (1960).
[36]G. Cunge, B. Crowley, D. Vender, and M. Turner, J. Appl. Phys. **89**, 3580 (2001).
[37]C.W. Chung, K.-I. You, S.H. Seo, S.S. Kim, and H.Y. Chang, Phys. Plasmas **8**, 2992 (2001).
[38]Yu.O. Tyshetskiy, A.I. Smolyakov, and V.A. Godyak, Plasma Sources Sci. Technol. **11**, 203 (2002).
[39]V.A. Godyak, B.M. Alexandrovich, and V.I. Kolobov, Phys. Rev. E **64**, 026406 (2001).
[40]Yu.M. Aliev, I.D. Kaganovich, and H. Shluter, Phys. Plasmas **4**, 2413 (1997).
[41]A. Smolyakov, V. Godyak, and Y. Tyshetskiy, Phys. Plasmas **8**, 3857 (2001).
[42]M. E. Jones, D. S. Lemons, R. J. Mason *et al.*, J. Comput. Phys. **123**, 169 (1996).